Nonlinear deformation analysis of a dielectric elastomer membrane–spring system

2010 Smart Mater. Struct. 19 085017

(http://iopscience.iop.org/0964-1726/19/8/085017)

Smart Mater. Struct. **19** (2010) 085017 (7pp) doi:10.1088/0964-1726/19/8/085017

Nonlinear deformation analysis of a dielectric elastomer membrane–spring system

Tianhu He[1], Leilei Cui[1], Cheng Chen[1] and Zhigang Suo[2]

[1] School of Science, Lanzhou University of Technology, Lanzhou 730050, People's Republic of China
[2] School of Engineering and Applied Sciences, Harvard University, Cambridge, MA 02138, USA

E-mail: heth@lut.cn

Received 6 November 2009, in final form 25 May 2010
Published 15 July 2010
Online at stacks.iop.org/SMS/19/085017

Abstract

Due to their large strain capability, dielectric elastomers are promising materials for application as transducers in cameras, robots, valves, pumps, energy harvesters, and so on. The dielectric elastomer transducers are based on the deformation of a soft polymer membrane contracting in thickness and expanding in area, induced by the application of a voltage across the two compliant electrodes coated on both sides of the membrane. This paper focuses on the static large deformation analysis of a dielectric elastomer membrane–spring system. The system is constructed from attaching a disk in the middle of a circular dielectric membrane and then connecting the disk with a spring. This configuration can be potentially used as a key part in valves. The basic governing equations describing the large out-of-plane deformations are formulated, and the obtained equations are solved numerically. The relations related to the displacement of the disk, the spring force, the applied voltage, and the parameters of spring including stiffness and initial length are illustrated. The results show that the anticipated displacement of the disk can be controlled by adjusting either or both of the parameters of the spring and the applied voltage. In addition, the parameters of the spring, that is, the stiffness and the initial length, play an important role in the performance of the membrane–spring system.

(Some figures in this article are in colour only in the electronic version)

1. Introduction

As a class of materials for electromechanical transduction, dielectric elastomers possess a unique combination of attributes: large deformation, fast response, high efficiency, low cost, and light weight [1–3]. These attributes make dielectric elastomers promising for applications as transducers in, for example, cameras, robots, and energy harvesters [4–8]. The essential part of such a transducer is a membrane of a dielectric elastomer. Subject to a voltage, the membrane reduces its thickness and expands its area, converting electrical energy into mechanical energy. Modeling dielectric elastomer transducers has been challenging due to the large deformation and nonlinear equations of state [9–12]. This paper explores these issues by studying a membrane of a dielectric elastomer deformed into an out-of-plane, axisymmetric shape (figure 1), a configuration used in a family of commercial devices known as universal muscle actuators (UMAs), marketed by Artificial Muscle, Inc. While many other configurations have been proposed in the literature, the focus on a particular configuration, such as the UMAs, may bring the benefits of standardization while still addressing a large range of early applications [13]. To focus our attention even further, this paper will be restricted to the fundamental issues of the electromechanics of membranes. In particular, attention here will be placed on a single membrane connected with a spring, as illustrated in figure 1, rather than the two membranes used in UMAs.

The study of axisymmetric deformation of membranes has a long tradition [14, 15]. Also studied recently

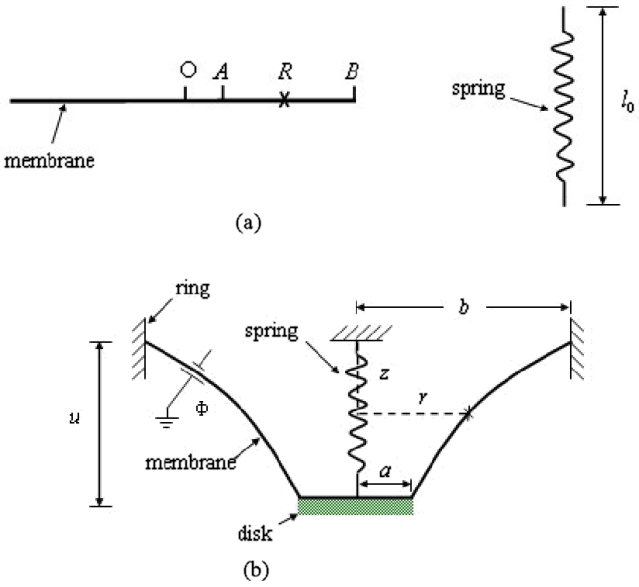

Figure 1. The cross section of an elastic membrane–spring system: (a) undeformed state; (b) deformed state.

is the axisymmetric deformation of membranes subject to electromechanical loads [16–18]. In this paper, we combine the nonlinear deformation field theory of membranes and the thermodynamics of elastic dielectrics. This approach follows the recent studies of elastic dielectrics [19–21]. Governing equations derived here recover those in [16] for an idealized material model, and can accommodate more general material models. We then describe numerical results for the specific configuration illustrated in figure 1. We show that the deformed membrane is curved due to the deformation in three dimensions, and the displacement of the disk can be controlled by altering either or both of the spring and the voltage.

2. State of equilibrium

Figure 1 illustrates the cross section of a dielectric elastomer membrane. A circular dielectric membrane is coated on both surfaces with compliant electrodes. In the undeformed state (figure 1(a)), the membrane is of thickness H and radius B.

A specific particle of the membrane is at a distance A from the center O, and a general particle is at a distance R from the center. In the deformed state (figure 1(b)), the membrane is well attached to a rigid disk of radius a, and to a rigid ring of radius b, and the disk is connected to a fixed spring with initial length l_0, such that particle A moves to place a, and particle B moves to place b. Meanwhile the membrane deforms into an out-of-plane, axisymmetric shape. Under the joint actions of the spring force F and the voltage Φ applied between the two electrodes, the disk moves relative to the ring by a distance u, and an amount of charge Q flows from one electrode to the other. Here, we focus on exploring the deformed configuration of the membrane–spring system under the actions of the spring force and the applied voltage. Thus, we ignore the weight of the rigid disk.

Following the work in [14], we first examine the kinematics of deformation. In the deformed state (figure 1(b)), the particle R moves to a place with coordinates r and z. The two functions, $r(R)$ and $z(R)$, fully describe the deformed shape, and are subject to the following boundary conditions, $r(A) = a$, $r(B) = b$, $z(B) = 0$. Consider the longitudinal stretch by examining two nearby particles, R and $R + \mathrm{d}R$. The two particles occupy places separated by $\mathrm{d}r = r(R + \mathrm{d}R) - r(R)$ and $\mathrm{d}z = z(R + \mathrm{d}R) - z(R)$. Let $\mathrm{d}l$ be the distance between the two particles when the membrane is in the deformed state, and $\theta(R)$ be the slope of the vector connecting the two particles, so that $\mathrm{d}r = \cos\theta\,\mathrm{d}l$, $\mathrm{d}z = -\sin\theta\,\mathrm{d}l$, and $(\mathrm{d}l)^2 = (\mathrm{d}r)^2 + (\mathrm{d}z)^2$. The longitudinal stretch is defined by the distance between the two particles in the deformed state divided by that in the undeformed state, $\lambda_1 = \mathrm{d}l/\mathrm{d}R$. In terms of the functions $r(R)$ and $z(R)$, the longitudinal stretch is

$$\lambda_1 = \sqrt{\left(\frac{\mathrm{d}r}{\mathrm{d}R}\right)^2 + \left(\frac{\mathrm{d}z}{\mathrm{d}R}\right)^2}. \tag{1}$$

Consider the latitudinal stretch by examining a circle of material particles, of perimeter $2\pi R$ in the undeformed state. In the deformed state, the circle of particles occupy a circle of places, of perimeter $2\pi r(R)$. Thus, the latitudinal stretch is

$$\lambda_2 = \frac{r}{R}. \tag{2}$$

We use nominal electric displacement to characterize the kinematics of charging. See [20] and [21] for a more general discussion. In the deformed state, let $\bar{D}$ be the nominal electric displacement, namely, the electric charge on an element of an electrode in the deformed state divided by the area of the element in the undeformed stated. Consequently, in the deformed state the total electric charge on the electrode is

$$Q = 2\pi \int \bar{D} R\,\mathrm{d}R. \tag{3}$$

Together, λ_1, λ_2, and $\bar{D}$ are the three kinematic variables that characterize the state of an element of the membrane. The membrane is also a thermodynamic system, taken to be held at a constant temperature. Let W be the Helmholtz free energy of an element of the dielectric in the deformed state divided by the volume of the element in the undeformed state. Consequently, the Helmholtz free energy of the entire membrane in the deformed state is $2\pi H \int W R\,\mathrm{d}R$. We stipulate that the free-energy density is a function of the three kinematic variables, $W(\lambda_1, \lambda_2, \bar{D})$.

When the kinematic variables vary by small amounts, the free-energy density varies by

$$\delta W = s_1\delta\lambda_1 + s_2\delta\lambda_2 + \bar{E}\delta\bar{D}. \tag{4}$$

This equation defines the three partial differential coefficients

$$s_1 = \frac{\partial W(\lambda_1, \lambda_2, \bar{D})}{\partial\lambda_1} \qquad s_2 = \frac{\partial W(\lambda_1, \lambda_2, \bar{D})}{\partial\lambda_2}$$
$$\bar{E} = \frac{\partial W(\lambda_1, \lambda_2, \bar{D})}{\partial\bar{D}}. \tag{5}$$

These partial differential coefficients can be readily interpreted from (4): s_1 is the longitudinal nominal stress, s_2 the latitudinal nominal stress, and $\bar{E}$ the nominal electric field. Once a free-energy function $W(\lambda_1, \lambda_2, \bar{D})$ is prescribed for a given material, (5) constitutes the equations of state.

We now combine the kinematics and thermodynamics to derive the field equations that govern the state of equilibrium. This approach avoids introducing the nebulous notion of electric body force; see [21] for further discussion. When the rigid disk moves by a small distance δu, the spring force does work $F\delta u$. When a small amount of charge δQ flows from one electrode to the other, the applied voltage does work $\Phi\delta Q$. In a state of equilibrium, thermodynamics dictates that, for arbitrary variation of the system, the change in the Helmholtz free energy of the membrane should equal the sum of the work done by the spring force and the applied voltage, namely

$$2\pi H \int_A^B \delta W R \, \mathrm{d}R = F\delta u + \Phi\delta Q. \tag{6}$$

Let the membrane be in a state of equilibrium characterized by $r(R)$, $z(R)$, and $\bar{D}(R)$, and let the state undergo a small variation characterized by $\delta r(R)$, $\delta z(R)$, and $\delta\bar{D}(R)$. From (1) we obtain the associated variation in the longitudinal stretch, $\delta\lambda_1 = \cos\theta \frac{\mathrm{d}(\delta r)}{\mathrm{d}R} - \sin\theta \frac{\mathrm{d}(\delta z)}{\mathrm{d}R}$. Using (4) and integrating by parts, we obtain that

$$\begin{aligned}\int_A^B \delta W R \, \mathrm{d}R &= (Rs_1 \cos\theta \delta r - Rs_1 \sin\theta \delta z)|_A^B \\ &+ \int_A^B \left[\left(-\frac{\mathrm{d}(Rs_1\cos\theta)}{\mathrm{d}R} + s_2\right)\delta r + \frac{\mathrm{d}(Rs_1\sin\theta)}{\mathrm{d}R}\delta z \right. \\ &\left. + R\bar{E}\delta\bar{D}\right]\mathrm{d}R. \end{aligned} \tag{7}$$

Comparing (6) and (7), and recalling that $\delta r(R)$, $\delta z(R)$, and $\delta\bar{D}(R)$ are independent variations, we obtain that

$$2\pi H R s_1 \sin\theta = F = k\Delta l \tag{8}$$

$$\frac{\mathrm{d}(Rs_1\cos\theta)}{\mathrm{d}R} = s_2 \tag{9}$$

$$H\bar{E} = \Phi. \tag{10}$$

In (8), $F = k\Delta l$ is spring force, and k is the stiffness of the spring, $\Delta l = l_0 - l$, and l is the length of the spring in the deformed state. Equations (8) and (9) can also be obtained by balancing forces in the directions of z and r, respectively, as done in [15]. Equation (10) recovers the definition of the nominal electric field.

3. Material model

To carry out numerical calculations, we need to prescribe an explicit form of the free-energy function $W(\lambda_1, \lambda_2, \bar{D})$. Here we adopt a material model [22], called the ideal dielectric elastomer, where the dielectric behavior is liquid-like, unaffected by deformation. Because our analysis is based on the static case, we neglect the time dependence of the material response. Specifically, the true electric displacement is linear in the true electric field, and the permittivity is independent of deformation. This material model seems to describe some experimental data [23], but is inconsistent with other experimental data [11, 12]. Nevertheless, this model has been used almost exclusively in previous analyses of dielectric elastomers. For a model of nonideal dielectric elastomers, see [19] and [24]. In what follows we develop results for the ideal dielectric elastomer.

The elastomer is assumed to be incompressible, so that the stretch in the thickness direction of the membrane, λ_3, relates to the longitudinal and latitudinal stretches as $\lambda_3 = 1/(\lambda_1\lambda_2)$. The thickness of the membrane is H in the undeformed state, and is $\lambda_3 H = H/(\lambda_1\lambda_2)$ in the deformed state. By definition, the true electric field E is the voltage divided by the thickness of the membrane in the deformed state, so that $E = \lambda_1\lambda_2\Phi/H = \lambda_1\lambda_2\bar{E}$. The true electric displacement D is defined as the charge in the deformed state divided by the area of the membrane in the deformed state, so that $D = \bar{D}/(\lambda_1\lambda_2)$.

For the ideal dielectric elastomer, following [25], we assume that the free-energy density takes the form

$$W(\lambda_1, \lambda_2, \bar{D}) = \frac{\mu}{2}(\lambda_1^2 + \lambda_2^2 + \lambda_1^{-2}\lambda_2^{-2} - 3) + \frac{\bar{D}^2}{2\varepsilon}\lambda_1^{-2}\lambda_2^{-2}. \tag{11}$$

The first term is the elastic energy, where μ is the small strain shear modulus. The second term is the dielectric energy, where ε is the permittivity. As seen in (11), the elastomer is taken to be a network of long and flexible polymers obeying the Gaussian statistics, so that the elastic behavior of the elastomer is neo-Hookean. For the ideal dielectric elastomer, the dielectric energy per unit volume is $D^2/2\varepsilon$, and the permittivity ε is a constant independent of deformation. In (11) the dielectric energy has been expressed in terms of the nominal electric displacement $\bar{D}$, a variable required by the function $W(\lambda_1, \lambda_2, \bar{D})$.

Inserting (11) into (5), we obtain the equations of state:

$$s_1 = \mu(\lambda_1 - \lambda_1^{-3}\lambda_2^{-2}) - \frac{\bar{D}^2}{\varepsilon}\lambda_1^{-3}\lambda_2^{-2} \tag{12a}$$

$$s_2 = \mu(\lambda_2 - \lambda_2^{-3}\lambda_1^{-2}) - \frac{\bar{D}^2}{\varepsilon}\lambda_2^{-3}\lambda_1^{-2} \tag{12b}$$

$$\bar{E} = \frac{\bar{D}}{\varepsilon}\lambda_1^{-2}\lambda_2^{-2}. \tag{12c}$$

Recall that the true stresses σ_1 and σ_2 relate to the nominal stresses as $\sigma_1 = \lambda_1 s_1$ and $\sigma_2 = \lambda_2 s_2$. We rewrite (12) in terms of the true quantities:

$$\sigma_1 = \mu(\lambda_1^2 - \lambda_1^{-2}\lambda_2^{-2}) - \varepsilon E^2 \tag{13a}$$

$$\sigma_2 = \mu(\lambda_2^2 - \lambda_2^{-2}\lambda_1^{-2}) - \varepsilon E^2 \tag{13b}$$

$$D = \varepsilon E. \tag{13c}$$

These equations are readily interpreted. For example, the first term in (12*a*) is the contribution to the stress due to the change of entropy associated with the stretch of the polymer network, and the second term is the contribution to the stress due to the applied voltage. Equation (13) in various forms has been used in previous analyses.

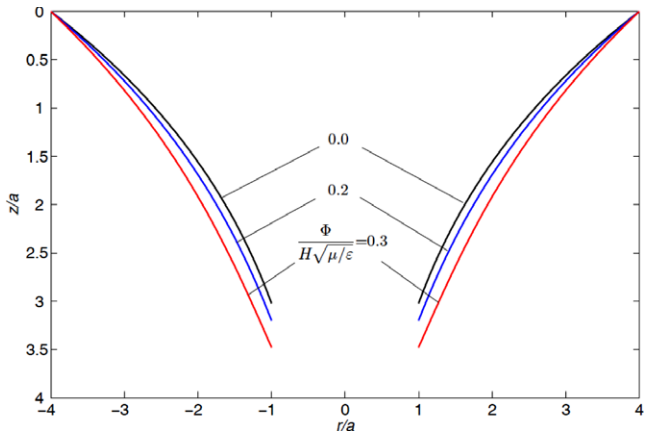

Figure 2. Deformed shapes of the membrane when the actuator is subject to several levels of voltage.

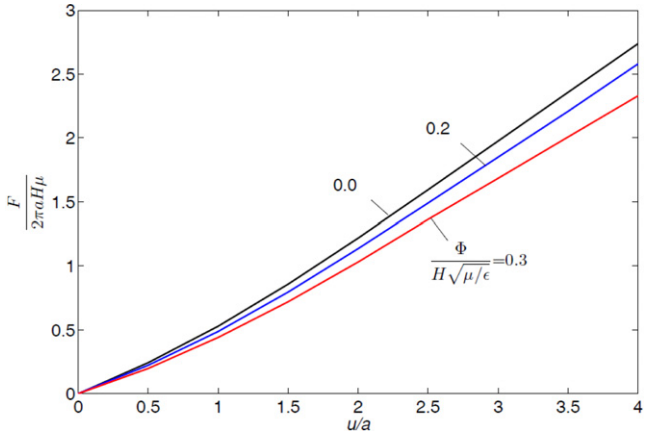

Figure 3. The relation between the spring force and the displacement of the attached disk under different voltages.

4. Numerical calculation and results

The theory presented above results in coupled nonlinear differential and algebraic equations, which we solve numerically; see the following for an outline of the method. For convenience, we normalize the following variables into dimensionless forms: H/a, u/a, L/a, $\Delta l/a$, $k/2\pi H\mu$, $Q/(2\pi a^2\sqrt{\varepsilon\mu})$, and $\Phi/(H\sqrt{\mu/\varepsilon})$. One can get the magnitude of the applied voltage from $\Phi/(H\sqrt{\mu/\varepsilon})$ when it is specified. For example, when $\Phi/(H\sqrt{\mu/\varepsilon}) = 0.2$, one obtains the applied voltage $\Phi = 2$ kV by using the representative values, $H = 100\ \mu$m, $\mu = 4\times10^5$ N m^{-2}, and $\varepsilon = 4\times10^{-11}$ F m^{-1}. Rewrite (1) as

$$\frac{\mathrm{d}r}{\mathrm{d}R} = \lambda_1\cos\theta. \tag{14}$$

A combination of (8) and (9) gives

$$\frac{\mathrm{d}\theta}{\mathrm{d}R} = -\frac{s_2}{s_1 R}\sin\theta. \tag{15}$$

The stresses in (15) are expressed using (12*a*) and (12*b*), which in turn are expressed as functions of r, λ_1, and Φ by using (2), (10), and (12*c*). Rewrite the algebraic equation (8) as

$$\left[1-\left(\frac{\Phi r}{R}\right)^2\right]\lambda_1^4 - \frac{F}{R\sin\theta}\lambda_1^3 - \left(\frac{R}{r}\right)^2 = 0. \tag{16}$$

In writing (16), we have normalized $F = k\Delta l$ and Φ.

Once the spring force $F = k\Delta l$ and the voltage Φ are prescribed, the ordinary differential equations (14) and (15), together with the algebraic equation (16), govern the three functions $r(R)$, $\theta(R)$, and $\lambda_1(R)$, subject to the boundary conditions $r(A) = a$, $r(B) = b$. The boundary value problem is solved by using the shooting method. Once $r(R)$ and $\theta(R)$ are solved, the function $z(R)$ is determined by integrating $\mathrm{d}z = -\tan\theta\,\mathrm{d}r$, subject to the initial condition $z(B) = 0$.

In designing a device using the configuration in figure 1, three dimensionless parameters can be varied: a/A, b/B, and b/a. We first fix the three parameters to specific values, $a/A = b/B = 1.2$, and $b/a = 4$. After numerical calculation, we get the results as shown in figures 2–9.

Figure 2 plots the cross section of the deformed shapes of the membrane. In the deformed state of the membrane–spring system as shown in figure 1(b), the spring undergoes compressive deformation, applying a downward reaction to the rigid disk. When the membrane tension induced by deformation is equal to the spring reaction, the membrane–spring system keeps balance at a certain position. It can be observed that the cross section of the membrane is curved due to the deformation in three dimensions, and the deformed shape is axisymmetric with respect to the axis along z-direction. When a voltage is applied between the two electrodes, the membrane reduces its thickness and expands its area because of Maxwell stress induced by electric field, thus, the disk lowers its position and enlarges its displacement. From figure 2, it can also be observed that the deformation of the membrane and the displacement of the disk increase with the applied voltage increasing.

Figure 3 plots the relation between the spring force and the displacement of the disk under different voltages. In figure 3, the zero value curve represents the static equilibrium position of the disk under the spring only. From figure 3, it can be observed that the disk can be lowered by increasing either or

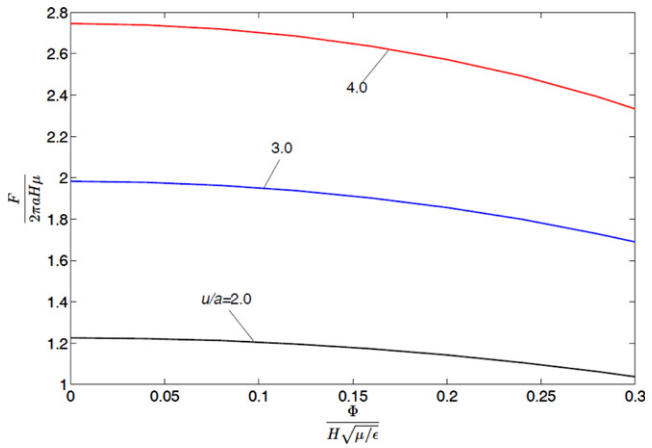

Figure 4. The relation between the spring force and the applied voltage under different displacements of the disk.

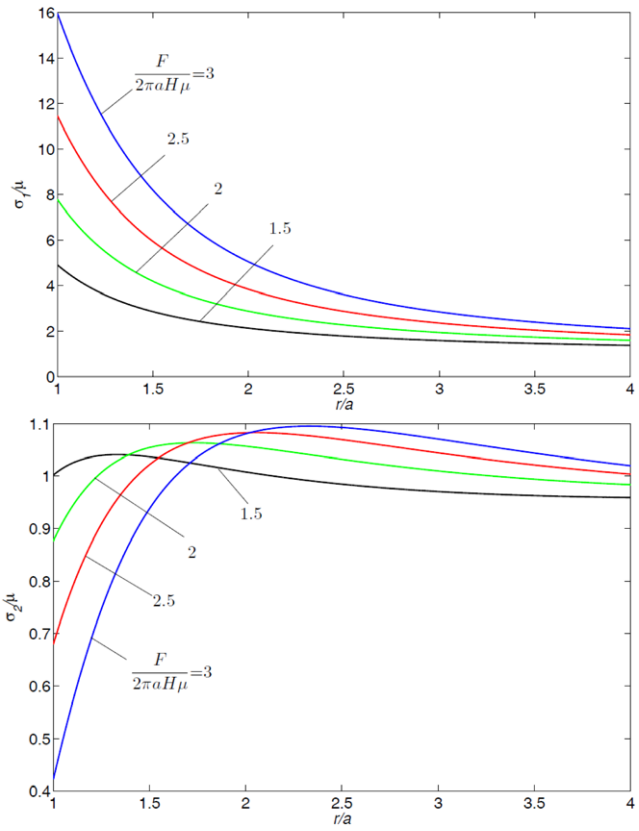

Figure 5. The distributions of the true stresses in the membrane when $\Phi/(H\sqrt{\mu/\varepsilon}) = 0.2$.

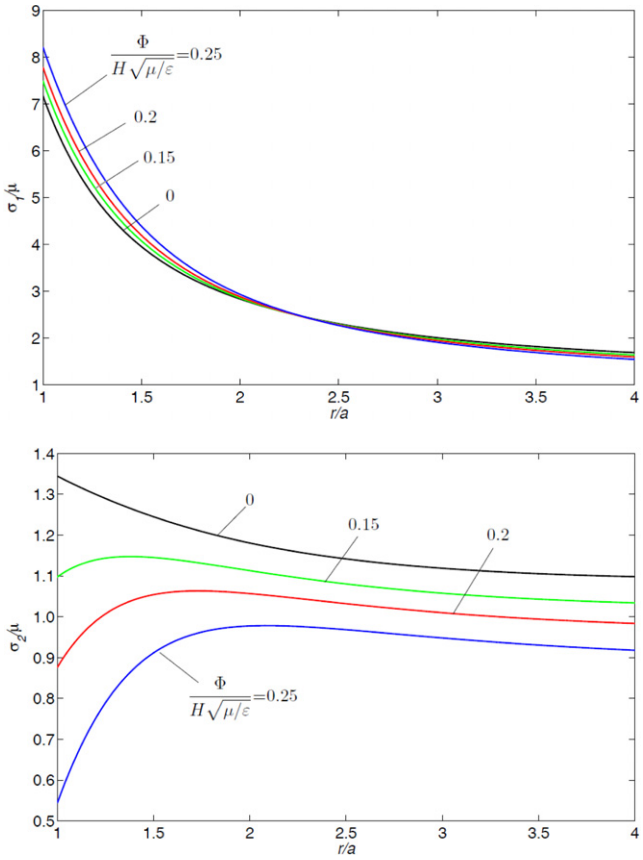

Figure 6. The distributions of the true stresses in the membrane when $F/2\pi aH\mu = 2$.

both of the applied voltage and the spring force. It can also be observed from figure 3 that in the case of either the spring force or the voltage being kept constant, the other should be increased if the disk needs to be lowered further.

Figure 4 plots the relation between the spring force and the applied voltage under different displacements of the disk. Figure 4 shows that if the displacement of the disk is kept fixed, the spring force and the applied voltage must match each other to maintain this fixed displacement. It implies that when the spring force goes up, the applied voltage must go down, and vice versa. Figure 4 also shows that the spring force has the major contribution to the displacement of the disk.

Figure 5 plots the distributions of the true stresses in the membrane for different spring forces when the applied voltage $\Phi/(H\sqrt{\mu/\varepsilon}) = 0.2$, and figure 6 plots the distributions of the true stresses in the membrane for different voltages when the spring force $F/2\pi aH\mu = 2$. To balance the applied spring force in the z direction, the longitudinal stress σ_1 is always tensile. The latitudinal stress σ_2, however, can become compressive when the applied voltage is large. This loss of tension may cause the membrane to buckle. Let $\sigma_2 = 0$, then one can calculate the critical voltage or the critical spring force. For example, in our calculation, we get the critical voltage is $\Phi/H\sqrt{\mu/\varepsilon} = 0.3034$ when the dimensionless spring force is specified as $F/2\pi aH\mu = 2$, while the critical spring force is $F/2\pi aH\mu = 3.653$ when the voltage is $\Phi/H\sqrt{\mu/\varepsilon} = 0.2$.

Figures 7–9 plot the relations between the displacement of the disk and the applied voltage when the disk has an initial

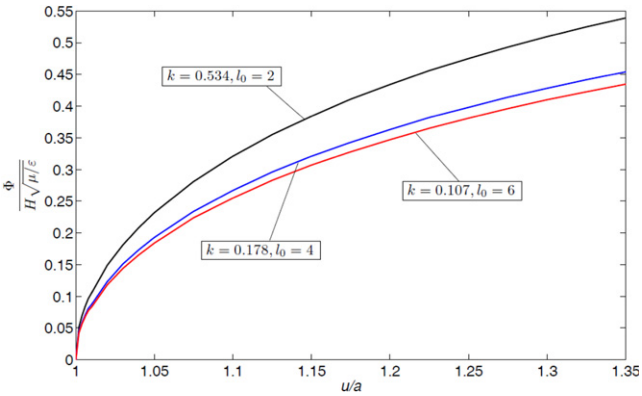

Figure 7. The relation between the displacement of the disk and the applied voltage when the disk has an initial displacement of $u/a = 1$.

displacement caused by the spring with no voltage. Here, we specify three different initial displacements for the disk, $u/a = 1$, $u/a = 1.5$, and $u/a = 1 = 2$. The spring has two parameters, the stiffness k and the initial length l_0, which can be altered to satisfy the specific performance requirements of the membrane–spring system. From figures 7 to 9, it can be found that for springs having the same initial length l_0, the one that has the largest stiffness k causes the largest initial displacement of the disk under the condition of applying no voltage. To attain the same initial displacement of the disk,

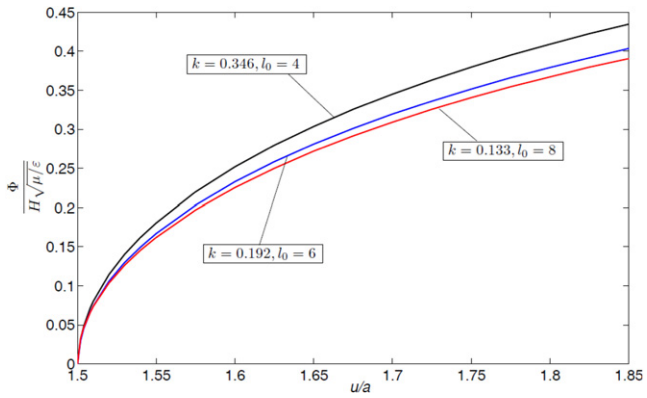

Figure 8. The relation between the displacement of the disk and the applied voltage when the disk has an initial displacement of $u/a = 1.5$.

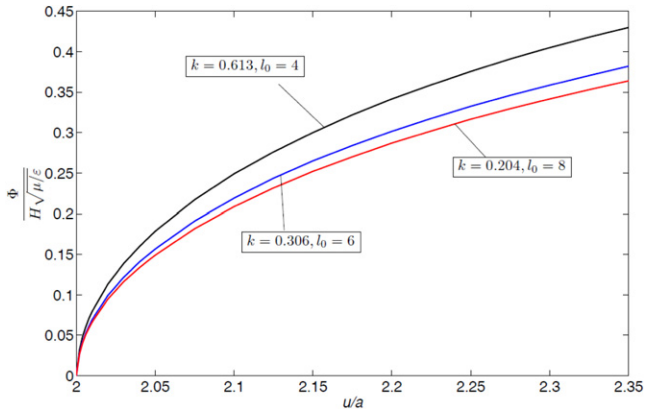

Figure 9. The relation between the displacement of the disk and the applied voltage when the disk has an initial displacement of $u/a = 2$.

the spring that has the smallest stiffness needs to have the largest initial length. It can also be observed from any one of figures 7–9 that when the voltage is kept fixed, the spring having larger initial length results in larger displacement of the disk. On the other hand, when the displacement of the disk is kept fixed, the applied voltage and the stiffness could be smaller in the case of the spring having larger initial length. As seen above, the parameters of the spring, that is, the stiffness and the initial length, play an important role in the performance of the membrane–spring system.

5. Conclusions

This paper focuses on the analysis of the static large deformation of a dielectric elastomer membrane–spring system. The nonlinear deformation field theory of dielectrics and the thermodynamics of the membrane–spring system were combined to derive the governing equations for the state of equilibrium. The shooting method was applied to solving the governing equations numerically. The obtained results show that the displacement of the disk can be controlled by altering either or both of the spring and the applied voltage. It can be concluded from the discussion on latitudinal stress that when the membrane–spring configuration functions as a value, the spring and the voltage need to maintain a delicate balance to avoid the membrane's buckle. The approach presented in this paper can be used to optimize the design of valves for specific applications.

Acknowledgments

This work was supported by the National Natural Science Foundation of China (10602021, 10872083) and China Postdoctoral Science Foundation (200902310). The authors gratefully acknowledge the support.

References

[1] Pelrine R, Kornbluh R, Pei Q B and Joseph J 2000 High-speed electrically actuated elastomers with strain greater than 100% *Science* **287** 836–9
[2] Pelrine R E, Kornbluh R D and Joseph J P 1998 Electrostriction of polymer dielectrics with compliant electrodes as a means of actuation *Sensors Actuators* A **64** 77–85
[3] Carpi F, Rossi D D, Kornbluh R, Pelrine R and Sommer-Larsen P 2008 *Dielectric Elastomers as Electromechanical Transducers: Fundamentals, Materials, Devices, Models and Applications of an Emerging Electroactive Polymer Technology* (Oxford: Elsevier)
[4] Bar-Cohen Y 2002 Electroactive polymers as artificial muscles: a review *J. Spacecraft Rockets* **39** 822–7
[5] Liu Y M, Ren K L, Hofmann H F and Zhang Q M 2005 Investigation of electrostrictive polymers for energy harvesting *IEEE Trans. Ultrason. Ferroelectr. Freq. Control* **52** 2411–7
[6] Wingert A, Lichter M D and Dubowsky S 2006 On the design of large degree-of-freedom digital mechatronic devices based on bistable dielectric elastomer actuators *IEEE-ASME Trans. Mech.* **11** 448–56
[7] Xia J Q, Ying Y R and Foulger S H 2005 Electric-field-induced rejection wavelength tuning of photonic bandgap composites *Adv. Mater.* **17** 2463
[8] Koford G, Wirges W, Paajanen M and Bauer S 2007 Energy minimization for self-organized structure formation and actuation *Appl. Phys. Lett.* **90** 081916
[9] Wissler M and Mazza E 2005 Modeling and simulation of dielectric elastomer actuators *Smart Mater. Struct.* **14** 1396–402
[10] Wissler M and Mazza E 2005 Modeling of a pre-strained circular actuator made of dielectric elastomers *Sensors Actuators* **120** 184–92
[11] Wissler M and Mazza E 2007 Mechanical behavior of an acrylic elastomer used in dielectric elastomer actuators *Sensors Actuators* **134** 494–504
[12] Wissler M and Mazza E 2007 Electromechanical coupling in dielectric elastomer actuators *Sensors Actuators* **138** 384–93
[13] Bonwit N, Heim J, Rosenthal M, Duncheon C and Beavers A 2006 Design of commercial applications of EPAM technology *Proc. SPIE* **6168** 39–48
[14] Adkins J E and Rivlin R S 1952 Large elastic deformations of isotropic materials: IX. The deformation of thin shells *Phil. Trans. R. Soc.* A **244** 505–31
[15] Tezduyar T E, Wheeler L T and Graux L 1987 Finite deformation of a circular elastic membrane containing a concentric rigid inclusion *Int. J. Non-Linear Mech.* **22** 61–72
[16] Goulbourne N, Mockensturm E and Frecker M 2005 A nonlinear model for dielectric elastomer membranes *ASME J. Appl. Mech.* **72** 899–906

[17] Mockendturm E M and Goulbourne N 2006 Dynamic response of dielectric elastomers *Int. J. Non-Linear Mech.* **41** 388–95
[18] Goulbourne N C, Mockensturm E M and Frecker M 2007 Electro-elastomers: large deformation analysis of silicone membranes *Int. J. Solids Struct.* **44** 2609–26
[19] McMeeking R M and Landis C M 2005 Electrostatic forces and stored energy for deformable dielectric materials *J. Appl. Mech.* **72** 581–90
[20] Dorfmann A and Ogden R W 2005 Nonlinear electroelasticity *Acta Mech.* **174** 167–83
[21] Suo Z G, Zhao X H and Greene W H 2008 A nonlinear field theory of deformable dielectrics *J. Mech. Phys. Solids* **56** 467–86
[22] Zhao X H, Hong W and Suo Z G 2007 Electromechanical coexistent states and hysteresis in dielectric elastomers *Phys. Rev.* **76** 134113
[23] Kofod G, Sommer-Larsen P, Kornbluh R and Pelrine R 2003 Actuation response of polyacrylate dielectric elastomers *J. Intell. Mater. Syst. Struct.* **14** 787–93
[24] Zhao X H and Suo Z G 2008 Electrostriction in elastic dielectrics undergoing large deformation *J. Appl. Phys.* **104** 123530
[25] Zhao X H and Suo Z G 2007 Method to analyze electromechanical stability of dielectric elastomers *Appl. Phys. Lett.* **91** 061921